Characteristics of YCoO3-type Perovskite Oxide and Application as an SOFC Cathode

Journal:	*Journal of Materials Chemistry A*
Manuscript ID	TA-ART-09-2020-009487.R1
Article Type:	Paper
Date Submitted by the Author:	19-Dec-2020
Complete List of Authors:	Sakai, Takaaki; National Institute of Advanced Industrial Science and Technology Tsukuba Center Tsukuba Central, Global zero emission research center Ogushi, Masako; Kyushu University Hosoi, Kohei; Kyushu University Inoishi, Atsushi; Kyushu university Hagiwara, Hidehisa; Kyushu University ida, Shintaro; Kyushu University Ooishi, Masatsugu; Tokushima University - Josanjima Campus Ishihara, Tatsumi; Kyushu University, Department of Applied chemistry Faculty of Engineering

SCHOLARONE™
Manuscripts

Characteristics of YCoO$_3$-type Perovskite Oxide and Application as an SOFC Cathode

Takaaki Sakai[a),b),c),*], Masako Ogushi[c)], Kohei Hosoi[c)], Atsushi Inoishi[d)], Hidehisa Hagiwara[c),e),1], Shintaro Ida[c),e),2], Masatsugu Oishi[f)], Tatsumi Ishihara[c),e)]

[a)] Global Zero Emission Research Center, National Institute of Advanced Industrial Science and Technology (AIST), 1-1-1 Higashi, Tsukuba, Ibaraki 305-8565, Japan

[b)] Center for Molecular Systems (CMS), Kyushu University, 744 Motooka, Nishi-ku, Fukuoka 819-0395, Japan

[c)] Department of Applied Chemistry, Faculty of Engineering, Kyushu University, 744 Motooka, Nishi-ku, Fukuoka 819-0395, Japan

[d)] Department of Advanced Device Materials, Institute for Materials Chemistry and Engineering, Kyushu University, 6-1 Kasugakouen, Kasuga, Fukuoka 816-8580, Japan

[e)] International Institute for Carbon Neutral Energy Research (WPI-I2CNER), Kyushu University, 744 Motooka, Nishi-ku, Fukuoka 819-0395, Japan

[f)] Graduate School of Technology, Industrial and Social Science, Tokushima University, Tokushima 770-8506, Japan

[1] Present affiliation of Hidehisa Hagiwara (co-author) is Hydrogen Isotope Research Center, Organization for Promotion of Research Center, University of Toyama, 3190 Gofuku, Toyama, 930-8555, Japan

[2] Present affiliation of Shintaro Ida (co-author) is Department of Applied Chemistry and Biochemistry, Graduate School of Science and Technology, Kumamoto University, 2-39-1 Kurokami, Chuo, Kumamoto 860-8555, Japan

* Corresponding author: Dr. Takaaki Sakai

Global Zero Emission Research Center, National Institute of Advanced Industrial Science and Technology (AIST), 1-1-1 Higashi, Tsukuba, Ibaraki 305-8565, Japan

tel: +81-29-861-8212

e-mail: sakai-takaaki@aist.go.jp

ABSTRACT

$YCoO_3$ is discussed as a novel cathode material for solid oxide fuel cells (SOFCs). One of the major issues for SOFC development is the side reactions that occur at the electrode and electrolyte interfaces. Characteristics such as the phase stability, reactivity against YSZ, electrical conductivity, and thermal expansion coefficients (TECs) of $YCoO_3$ were investigated. $YCoO_3$ was produced by the sol-gel method below 975 °C, and the least impurities were observed at a Y molar ratio of 0.96 (YCO-096). YCO-096 did not react significantly with the YSZ electrolyte when fired at 975 °C for 1 h. The main charge carrier of YCO-096 was confirmed to be electron-holes, h^+, and the maximum conductivity was estimated to be 700 S cm^{-1} at 900 °C. The TECs of YCO-096 were in the range of 16.5–44.2×10^{-6} °C^{-1} from room temperature to 900 °C. The YCO-096 cathode was stable in the YSZ electrolyte SOFC. Oxygen defects formed at the surfaces of particle YCO-096 were considered to significantly improve the cathodic performance.

Introduction

Solid oxide fuel cells (SOFCs) have recently received considerable attention due to their higher energy efficiency than other fuel cells. In this electrochemical device, a zirconia-based oxide ion conductor such as yttria-stabilized zirconia (YSZ) [1,2] or Scandia-stabilized zirconia (ScSZ) [3,4] with a higher ion conductivity at around 800 °C is often used as the electrolyte. YSZ has been most frequently selected as the electrolyte for commercially available SOFCs due to its cost advantage, although its ionic conductivity is inferior to that of ScSZ. However, the critical problem of the ZrO_2 based oxide is reactivity with La cobaltite-based perovskite oxides, which are commonly used as cathode materials due to their excellent electrode performance [5-8]. ZrO_2 easily reacts with La or alkaline earth elements contained in these materials and forms an impurity phases such as lanthanoid pyrochlore ($La_2Zr_2O_7$) or alkaline earth perovskites ($Re ZrO_3$) at higher temperatures [9-12]. CeO_2 based oxides such as gadolinium doped ceria (GDC) are introduced between the YSZ electrolyte and cathode as an interlayer to prevent this reaction. However, the introduction of a CeO_2 interlayer causes another problem because the CeO_2 based oxide easily reacts with YSZ and forms a solid solution, which leads to a significant decrease in the ionic conductivity of YSZ [13]. Therefore, the development of a cathode material with less reactivity toward ZrO_2 based electrolyte is desirable to further improve the SOFC performance. A new cathode material that does not utilize any alkaline earth element has been reported; the $LaCo_{1-x}Ni_xO_{3-\delta}$ series oxides exhibit relatively high cathode performance [14,15]. However, the problem with the use of La cannot be solved by this material, because a large amount of La is still contained in the A sites of the perovskite structure. The substitution of other lanthanoid

elements for La also cannot solve the reactivity problem, because the current La based cathode is the most stable toward the ZrO_2 electrolyte, as shown in Fig. S1; all lanthanoid type cobaltites inevitably form the pyrochlore phase (or $Ln_4Zr_3O_{12}$ phase [16]) during the typical cathode firing at around 1000 °C and the problem of reactivity cannot be avoided. Aside from the lanthanoid cobaltites, yttrium cobaltite ($YCoO_3$) (YCO) has been reported as a magnetic material or thermoelectric material [17,18]. There is a possibility that YCO has low reactivity toward YSZ because Y is already contained in its structure. In addition, even if YCO only reacted slightly with the YSZ electrolyte, it is considered that its influence on the electrolyte would not be severe, because only the amount of Y doping would increase slightly.

Here, YCO was synthesized and its phase stability, reactivity toward YSZ, electrical conductivity, and thermal expansion coefficient (TEC), which are important features as an SOFC cathode, were investigated. YCO was also applied to a YSZ electrolyte based SOFC and its cathode properties were investigated.

Experimental

Sample preparation

YCO oxide was synthesized by the sol-gel method using $Y(NO_3)_3 \cdot 6H_2O$ (Kishida Chemical Co., Ltd.), $Co(NO_3)_2 \cdot 6H_2O$ (Kishida Chemical Co., Ltd.), and citric acid (Wako Pure Chemical Industries, Ltd.). The water content of these nitrates was confirmed by thermogravimetry (TG-8120, Rigaku Corp.). The starting materials were dissolved in distilled water at a molar ratio of 1:1:2, and stirred and heated with a hot stirrer until the water in the solution was fully evaporated. The obtained precursor was calcined at 400 °C for 2 h in air to remove NO_x. After calcination, the resultant product

was ground with a mortar and pestle and calcined at 900–1000 °C for 20 h in air to obtain the YCO powder. For the electrical conductivity, Seebeck coefficient, and TEC measurements, bar-type samples were prepared by the following procedure. YCO powder was molded into pellets, cold isostatically pressed at 300 MPa, sintered at 975 °C for 20 h, and cut into bar-shaped specimens with a diamond cuter. The cathode performance of the YCO powder was tested with 8 mol% Y_2O_3-ZrO_2 (8YSZ) electrolyte and Ni-$Ce_{0.8}Sm_{0.2}O_{2-\delta}$ (Ni/SDC) anode. An 8YSZ electrolyte pellet was prepared by molding commercially available 8YSZ powder (TZ-8Y, Tosoh Corp.) into a disk shape, cold isostatically pressing at 300 MPa, sintering at 1500 °C for 10 h, and polishing with #2000 abrasive paper. The thickness of the 8YSZ electrolyte was ca. 0.3 mm. Ni/SDC anode paste was prepared by mixing NiO (Wako Pure Chemical Industries, Ltd.) and SDC (SDC20, Daiichi Kigenso Kagaku Kogyo, Co., Ltd.) in a ratio of 90:10 (wt%), ball-milling at 300 rpm for 1 h in ethanol with 15 mm zirconia balls, and processing into a paste with ethyl cellulose at a weight ratio of 100:6 and mixing with a thinner. The YCO powder was also ball-milled and processed into a paste by a similar procedure. The particle size of YCO-096 was several micrometers, as shown in Fig. S2. The anode and cathode pastes were then screen-printed onto the YSZ electrolyte. The diameter of the electrodes was ca. Φ5 mm (= 0.2 cm^2) and the amount was ca. 10 mg cm^{-2} to achieve sufficient current collection properties [11].

Characterization

    The crystal structure of the synthesized YCO powder was confirmed using X-ray diffraction (XRD; RINT-2000, Rigaku Corp.) with Cu-K_α radiation. Electrical conductivity measurements were performed using the conventional DC 4-probe method

with a commercially available Pt electrode (TR-7907, Tanaka K.K. Corp.) and a thermoelectric property measurement system (RZ2001i, Ozawa Kagaku Corp.). The Seebeck coefficient was also measured during the conductivity measurement. TEC was measured with a dilatometer (DIL-40C, NETZSCH Gerätebau GmbH) and an Al_2O_3 type sample holder by scanning the temperature from room temperature (R.T.) to 900 °C at a rate of 2 °C min^{-1}.

The experimental apparatus for the SOFC power generation test using the YCO cathode is shown in Fig. S3. The cell was sandwiched with pyrex glass sealing rings and heated at 975 °C for 1 h to fire the electrodes before the power generation test. O_2 gas was introduced to the YCO cathode at 30 mL min^{-1} during the firing process. For the power generation test, humidified H_2 gas at R.T. (about 3%H_2O-H_2 gas) and 100%O_2 gas were introduced to the anode and cathode compartments at a flow rate of 100 mL min^{-1}, respectively. The cathode impedance was measured using an electrochemical impedance analyzer (Solartron 1287+1260, Ametek Inc.,), and the power generation test was performed using a potentio/galvanostat (HA-151B, Hokuto Denko Corp.).

Results and discussion

Figure 1 shows XRD patterns of the YCO (YxCoO$_{3-\delta}$, $0.9 < x < 1.0$) oxides synthesized at 925 °C for 20 h. The XRD pattern of YCO ($x = 1.0$) revealed peaks that were mainly attributed to those of the YCO perovskite, of which the structure is an orthorhombic type (space group: *Pmna*). However, as shown in Fig. 3(b), a small peak was observed at around 29°, which corresponds to the main peak of Y_2O_3 and indicates that the sample obtained contained trace Y_2O_3 as a secondary phase. Thus, to decrease this secondary phase, the content of Y was decreased up to 0.9, as shown in Fig. 1. In

addition, this introduction of Y defect was also aimed at the increase of the amount of oxide ion vacancies, which would increase the cathode performance of YCO

Even though the Y_2O_3 peak seemed to decease slightly with the amount of Y, a peak attributed to Co_3O_4 appeared and it increased for Y contents of 0.96 and less, as shown in Fig. 1(c). It is likely that the elimination of secondary phases by changing the amount of Y is difficult for the YCO oxide and the composition around Y = 0.96 contained the least secondary phases. Therefore, $Y_{0.96}CoO_{3-\delta}$ (YCO-096) was mainly evaluated for subsequent measurements.

Figure 2 shows the thermal stability of YCO-096 confirmed by XRD. YCO-096 was treated at 900 to 1000 °C for 20 h in air. YCO-096 decomposed to Y_2O_3 and Co_3O_4 at around 1000 °C, and a similar tendency was also reported by Feng et al. [17]. This result suggests that YCO oxide is thermodynamically unstable at higher temperature and should be used below 1000 °C.

To confirm the reactivity of YCO-096 with YSZ, YCO-096 powder was mixed with 8YSZ powder in a weight ratio of 1:1 using mortar and pestle, and the mixture was heat-treated at 950 or 975 °C for 1 h in air. The 8YSZ powder was calcined at 1500 °C before mixing with the YCO-096 powder. Figure 3 shows XRD patterns of the mixtures before and after the heat treatment. The main peak of Co_3O_4 should increase when the Y in the YCO oxide reacts with 8YSZ; however, the main peak of Co_3O_4 was significantly small in both cases. This result indicates that the reactivity of YCO-096 with 8YSZ was low and the reaction did not readily proceed, even at the typical electrode firing temperature around 1000 °C. After treatment at 975 °C for 100 h, as shown in Fig. S4, reaction of the powders was clearly observed. The peak of Co_3O_4 was observed at 37°,

and a slight peak that may be attributed to a Y-rich phase was also observed at the shoulder of the main YSZ peak. However, heat treatment for 100 h is not a typical condition for the electrode firing process.

Figure 4 shows the electrical conductivity of YCO-096 measured by the DC 4-probe method. The conductivity of YCO-096 was less than 10^{-3} S cm^{-1} at R.T., but suddenly increased at 300–600 °C and was eventually ca. 10^2 S cm^{-1} at 800 °C. A similar sudden increase in conductivity was observed for LaCoO$_3$ [19]. Tagawa et al. reported that the electrical conductivity varies with the relative density of the sample; therefore, the electrical conductivity was calibrated with respect to the relative density using a calibration equation [20]. The maximum electrical conductivity of YCO-096 reached 700 S cm^{-1} at 900 °C, as shown in Fig. 4.

Figure 5 shows the Seebeck coefficient of YCO-096 measured from R.T. to 900 °C. The Seebeck coefficient of YCO-096 was positive, which suggests the main charge carrier is electron-holes, h$^+$. The Seebeck coefficient at around R.T. was as high as 1700 µV K^{-1}, which indicates that the charge carrier density of YCO-096 at a lower temperature is significantly small. Therefore, the low electrical conductivity of YCO-096 at lower temperature is attributed to the low charge carrier density. In addition, the Seebeck coefficient suddenly increased at 300–600 °C, which also indicates that the charge carrier density increased significantly in this temperature range, which is consistent with the sudden increase in the conductivity observed. There are two possibilities for the increase in the carrier density. One is that oxide ion vacancies are filled with oxygen when the temperature increases, which would lead to an increase in the electron-hole concentration (Eq. (1)). The other is a change in the valence of the cobalt ion from 3+ to 2+ as the temperature increases (Eq. (2)).

$$V_O^{\bullet\bullet} + \tfrac{1}{2}O_2 \rightarrow O_O^{x} + 2h^{\bullet} \hspace{4cm} (1),$$

$$Co_{Co}^{x} \rightarrow Co_{Co}' + h^{\bullet} \hspace{4cm} (2),$$

where $V_O^{\bullet\bullet}$ is an oxide ion vacancy, O_O^{x} is an O^{2-} ion in the lattice of YCO, Co_{Co}^{x} and Co_{Co}' are Co^{3+} and Co^{2+} in the lattice of YCO, and $h^{\bullet}$ is an electron-hole, h^{+}. The oxygen vacancies of perovskite oxides generally increase with the temperature [21-23]; therefore, the former reaction is unlikely to occur in the perovskite oxide. The latter reaction may thus explain the increase in the charge carrier density.

Figure 6 shows the TEC of YCO-096 as a function of temperature. The TEC increased at around 300–600 °C, the range of which is similar to the variations observed in the electrical conductivity and Seebeck coefficient. The ionic radius of Co^{2+} is larger than that of Co^{3+}, so that this result also supports the possibility of a valence change of the Co ion in YCO-096. The TECs of YCO-096 at various temperatures are summarized in Table 1. The TECs of YCO-096 are significantly larger than that of 8YSZ, of which the TEC is typically 10×10^{-6} °C^{-1} [24], which is consistent with the high TECs that are often observed for cobaltite-based oxides.[25] The high TEC of YCO-096 is thus problematic for practical application.

Figure 7 shows IV and IP curves for the YCO-096|8YSZ|Ni/SDC cell operated at 800 °C. Stable IV and IP curves were obtained using the YCO-096 cathode, which indicates that YCO is stable and applicable as an SOFC cathode. However, the cell voltage rapidly decreased in the low current bias region (within 100 mAcm^{-2} = 20 mA) of the IP curve. In this case, the voltage change by the water vapor pressure is estimated

at less than 3 mV, and it is unlikely that this voltage drop was caused by the water vapor pressure change produced by the power generation. Thus, this result suggests that the performance of the YCO-096 cathode requires a certain bias voltage for activation. The electrochemical impedance spectroscopy results shown in Fig. S5 also indicate considerable activation of the YCO-096 cathode by a cathodic bias. It is well known that the main rate-determining step of the electrode reaction is the surface diffusion of adsorbed oxygen species [26,27]. There is a strong possibility that the cathodic bias produced the oxide ion vacancies, $V_O^{\bullet\bullet}$, and the produced $V_O^{\bullet\bullet}$ would enhance the surface adsorption and diffusion of oxygen species, which resulted in a significant activation of the cathode performance.

The present results showed that the YCO cathode is stable in the YSZ based cell. The introduction of more oxygen defects in YCO would be expected to further improve the cathode performance.

Conclusion

YCO was synthesized by the sol-gel method and the phase stability, reactivity toward YSZ, electrical conductivity, and the TECs were investigated. Orthorhombic perovskite-type YCO was obtained below 975 °C, even though a small amount of impurities such as Y_2O_3 and Co_3O_4 remained. The least impurities were observed when the Y molar ratio was 0.96 ($Y_{0.96}CoO_{3-\delta}$, YCO-096). YCO-096 did not readily react with the YSZ electrolyte when fired at 975 °C for 1 h. Electrical conductivity and Seebeck coefficient measurements indicated that the main charge carrier of YCO-096 was electron-holes, and a maximum conductivity of 700 S cm^{-1} was observed at 900 °C.

The TECs of YCO-096 were in the range of 16.5–44.2×10^{-6} °C^{-1} from R.T. to 900 °C. YCO-096 was used as the cathode with an 8YSZ electrolyte cell. The YCO-096 cathode was stable during cell operation and showed significant activation under a cathodic bias, which was attributed to an increase in oxide ion vacancies on the YCO-096 surface.

Acknowledgements

Conflict of interest

There are no conflicts to declare.

Notes and References

1. E.C. Subbarao, Solid Electrolytes and Their Applications, Plenum Press, New York, 1980.

2. J.-H. Park and R. N. Blumenthal, *J. Electrochem. Soc.*, 1989, 136, 2867-2876.

3. D.W. Stricker and W.G. Carlson, *J. Am. Ceram. Soc.*, 1965, 48, 286-289.

4. O. Yamamoto, Y. Arati, Y. Takeda, N. Imanishi, Y. Mizutani, M. Kawai and Y. Nakamura, *Solid State Ionics*, 1995, 79, 137-142.

5. Y. Takeda, R. Kanno, M. Noda, Y. Tomida and O. Yamamoto, *J. Electrochem. Soc.*, 1987, 134, 2656-2661

6. S. B. Adler, *Solid State Ionics,* 1998, 111, 125-134.

7. L.-W. Tai, M.M. Nasrallah, H.U. Anderson, D.M. Sparln and S.R. Sehlin, *Solid State Ionics*, 1995, 76, 259-271

8. L.-W. Tai, M.M. Nasrallah, H.U. Anderson, D.M. Sparln and S.R. Sehlin, *Solid State Ionics*, 1995, 76, 273-283.

9. H. Yokokawa, N. Sakai, T. Kawada and M. Dokiya, *DENKI KAGAKU*, 1989, 57, 821-828.

10. M. Sase, D. Ueno, K. Yashiro, A. Kaimai, T. Kawada and J. Mizusaki, *J. Phys. Chem. Solids*, 2005, 66, 343-348.

11. J. Mizusaki, H. Tagawa, K. Tsuneyoshi, K. Mori and A. Sawata, *NIHONKAGAKUKAISHI*, 1988, 1623-1629.

12. L. Kindermann, D. Das, H. Nickel and K. Hilpert, *Solid State Ionics*, 1996, 89, 215-220.

13. H. Naito, N. Sakai, T. Otake, H. Yugami and H. Yokokawa, *Solid State Ionics*, 200, 135, 669-673.

14. R. Kiebach, P. Zielke, S. Veltz, S. Ovtar, Y. Xu, S. B. Simonsen, K. Kwok, H. L. Frandsen and R. Kungas, *J. Electrochem. Soc.*, 2017, 164, F748-F758.

15. X.-K. Gu, J. S. A. Carneiro, S. Samira, A. Das, N. M. Ariyasingha and E. Nikolla, *J. Am. Chem. Soc.*, 2018, 140, 8128-8137.

16. M. Salazar-Zertuche, J. A. Diaz-Guillen, J. O. Acosta-García, J. C. Diaz-Guillen, S. M. Montemayor, O. Burciaga-Diaz, M. E. Bazaldua-Medellin and A. F. Fuentes, *Int. J. Hydrogen Energy*, 2019, 44, 12500-12507.

17. G. Feng, Y. Xue, H. Shen, S. Feng, L. Li, J. Zhou, H. Yang and D. Xu, *Phys. Status Solidi A*, 2012, 209, 1219-1224.

18. L. Yi, L. Hai-Jin, Z. Qing, L. Yong and L. Hou-Tong, *Chin. Phys. B*, 2013, 22,

057201.

19. J. Mizusaki, J. Tabuchi, T. Matsuna, S. Yamaguchi and K. Fueki, *Proc. Symp. Electro-ceramics and Solid State Ionics*, 1988, 88-3, 95-103.

20. H. Tagawa, J. Mizusaki, Y. Arai, Y. Kuwayama, S. Tsuchiya, T. Takeda and S. Sekido, *DENKI KAGAKU*, 1990, 58, 512-519.

21. M. Kuhn, S. Hashimoto, K. Sato, K. Yashiro and J. Mizusaki, *J. Solid State Chemistry*, 2013, 197, 38-45.

22. M. Kuhn, Y. Fukuda, S. Hashimoto, K. Sato, K. Yashiro and J. Mizusaki, *J. Electrochem. Soc.* 2012, 160, F34-F42.

23. S. Miyoshi, J.-O. Hong, K. Yashiroa, A. Kaimaia, Y. Nigaraa, K. Kawamura, T. Kawada and J. Mizusakia, *Solid State Ionics*, 2003, 161, 209-217.

24. M. Mori, T. Yamamoto, H. Itoh, H. Inaba and H. Tagawa, *J. Electrochem. Soc.*, 1998, 145, 1374-1381.

25. K. Knizek, Z. Jirak, J. Hejtmanek, M. Veverka, M. Marysko, G. Maris and T.T.M. Palstra, *Eur. Phys. J. B*, 2005, 47, 213-220.

26. J. Mizusaki, K. Amano, S. Yamauchi and K. Fueki, *Solid State Ionics*, 1987, 22, 313-322.

27. J. Mizusaki, K. Amano, S. Yamauchi and K. Fueki, *Solid State Ionics*, 1987, 22 323-330.

Figure captions

Fig. 1. XRD patterns of $Y_xCoO_{3-\delta}$ synthesized by the sol-gel method ($0.9 \leq x \leq 1.0$). (a) XRD patterns from 10° to 80°, (b) magnified patterns from 27° to 31°, and (c) magnified patterns from 35° to 38°.

Fig. 2. XRD patterns of $Y_{0.96}CoO_{3-\delta}$ after heating at various temperatures for 20 h.

Fig. 3. XRD patterns for a mixture of $Y_{0.96}CoO_{3-\delta}$ and YSZ-8 heated at 950 and 975 °C for 1 h. The weight ratio of the YCO-YSZ mixture was 1:1. (a) XRD patterns from 10° to 80° and (b) magnified patterns from 35° to 39°.

Fig. 4 Electrical conductivity of $Y_{0.96}CoO_{3-\delta}$ measured by DC 4 probe method under ambient air (P_{O2} = 0.21 atm); the closed symbols are raw data and the open symbol are the conductivity calibrated by the effect of the relative density.

Fig. 5. Seebeck coefficient of $Y_{0.96}CoO_{3-\delta}$ measured from R.T. to 900 °C in air (P_{O2} = 0.21 atm).

Fig. 6. Thermal expansion curve of $Y_{0.96}CoO_{3-\delta}$ measured from R.T. to 900 °C in air at a scan rate of 2 °C min^{-1}.

Fig. 7. IV and IP curves of the YCO cathode for a Ni/SDC|YSZ|YCO cell measured at 800 °C.

Table 1 TECs of $Y_{0.96}CoO_{3-\delta}$ calculated from the thermal expansion rate.
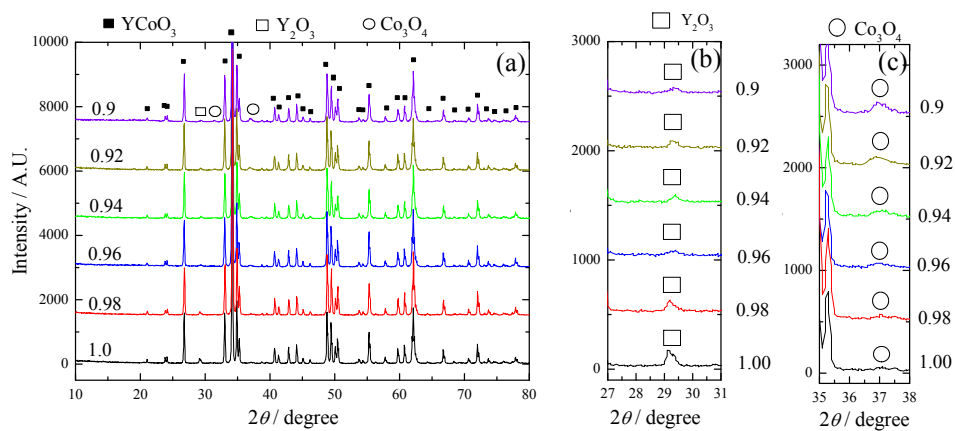
Fig. 1 XRD pattern of $Y_xCoO_{3-\delta}$ synthesized by sol-gel method ($0.9 \leq x \leq 1.0$). XRD pattern from 10 to 80 degree (a), magnified pattern from 27 to 31 degree (b) and magnified pattern from 35 to 38 degree (c).
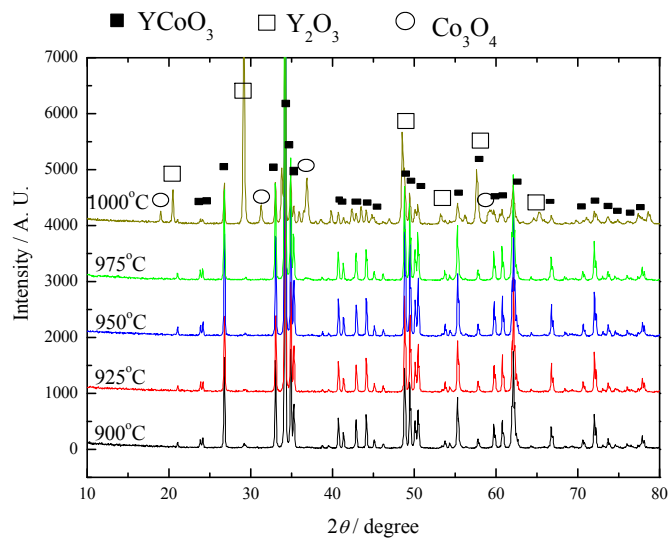
1

Fig. 2 XRD pattern of the $Y_{0.96}CoO_{3-\delta}$ after heated at respective temperature for 20 h.
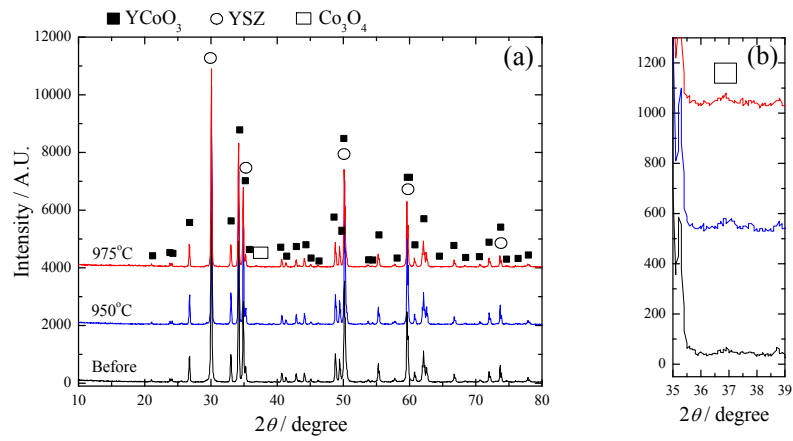
Fig. 3 XRD pattern of the mixture of $Y_{0.96}CoO_{3-\delta}$ and YSZ-8 heated at respective temperature for 1h. The weight ratio of the YCO-YSZ mixture is 1:1. XRD pattern from 10 to 80 degree (a) and magnified pattern from 35 to 39 degree (b).
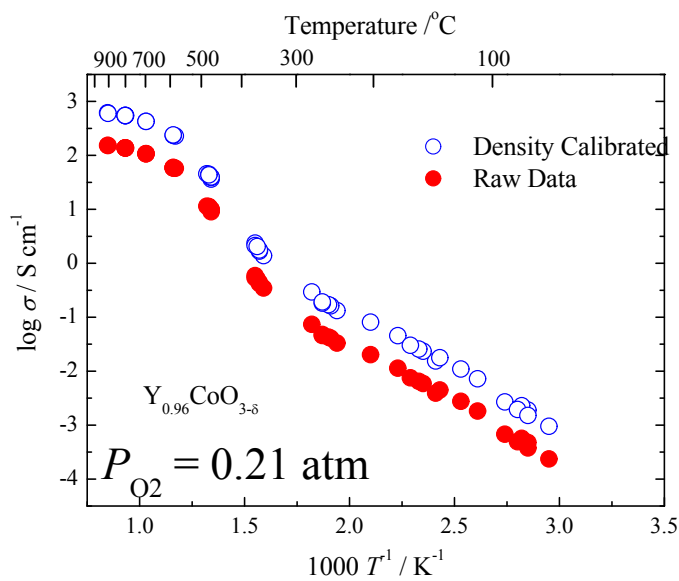
Fig. 4 Electrical conductivity of $Y_{0.96}CoO_{3-\delta}$ measured by DC 4 probe method under ambient air (P_{O2} =0.21 atm); the closed symbols are raw data and the open symbol are the conductivity calibrated by the effect of the relative density.
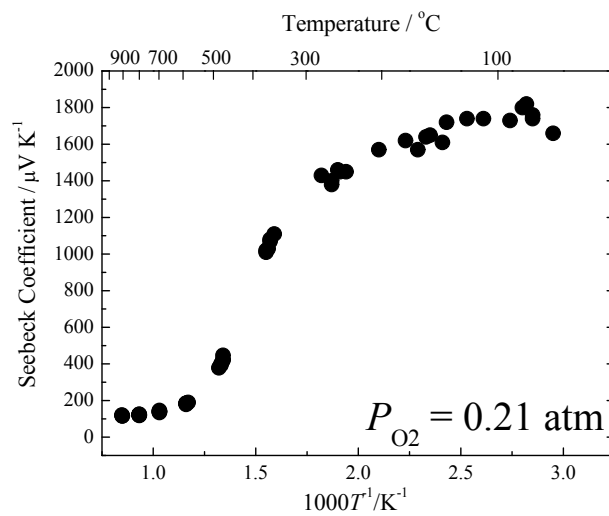
Fig. 5 Seebeck coefficient of $Y_{0.96}CoO_{3-\delta}$ measured from R.T. to 900°C in air (P_{O2} = 0.21 atm).
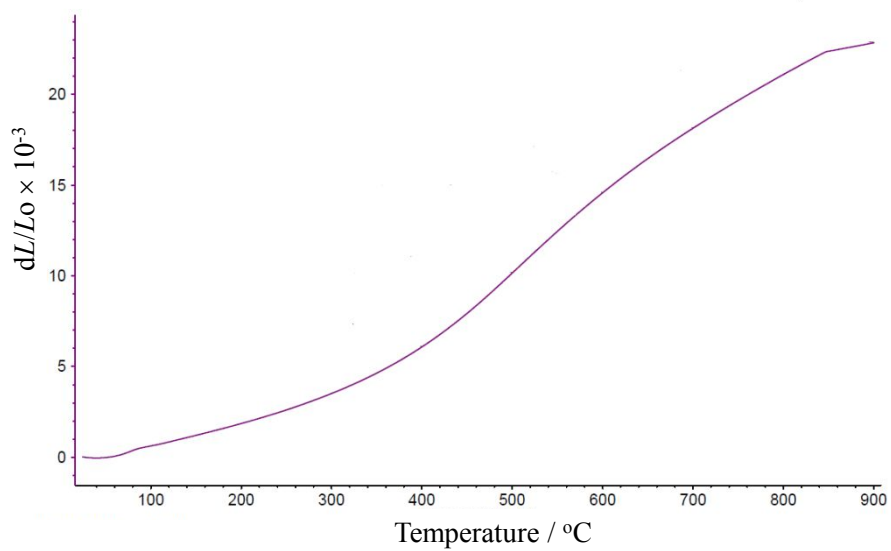
Fig. 6 Thermal expansion curve of $Y_{0.96}CoO_{3-\delta}$ measured from R.T. to 900°C in air at the
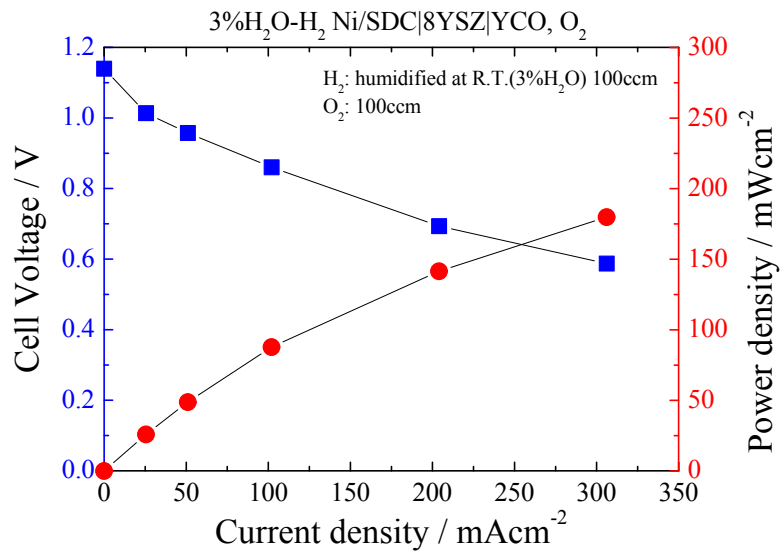
scan rate of 2°C/min.

Fig. 7 IV curve and IP curve of the YCO cathode of the Ni/SDC|YSZ|YCO cell measured at 800°C.

Table 1 Thermal expansion coefficient (TECs) of $Y_{0.96}CoO_{3-\delta}$ calculated from the thermal expansion rate.

Temperature / °C	TEC / °C^{-1}
200-300	16.5×10^{-6}
300-400	25.7×10^{-6}
400-500	40.7×10^{-6}
500-600	44.2×10^{-6}
600-700	35.6×10^{-6}
700-800	29.6×10^{-6}
800-900	17.4×10^{-6}

Graphical abstract